P. Rama Lakshmi, Dr P.Ravinder Reddy / International Journal of Engineering Research and Applications (IJERA) ISSN: 2248-9622 www.ijera.com
Vol. 2, Issue 3, May-Jun 2012, pp.001-010

Investigation of interlaminar shear strength in carbon epoxy and carbon epoxy carbon nanotubes using experimental and finite element technique

P. Rama Lakshmi * and Dr P.Ravinder Reddy**

* Research Scholar, Department of Mechanical Engineering,
Jawaharlal Nehru Technological University,
Hyderabad

** Professor and Head, Department of Mechanical Engineering,
Chaitanya Bharathi Institute of Technology, Gandipet, Hyderabad

ABSTRACT

The present study concerns experimental and finite element analysis of carbon epoxy and carbon epoxy carbon nanotube composites to estimate interlaminar shear strength. Mechanical properties such as elastic ratios, thickness are varied for double notched specimen and the corresponding deflections and interlaminar shear strengths are estimated by ANSYS. From simple rule of mixtures, equivalent orthotropic material properties are estimated. These properties are provided as input in ANSYS to generate finite element model. Solid layered element is used to model double notch specimen. To estimate the properties of carbon epoxy carbon nanotube composite, initially finite element model of matrix and carbon nanotube is generated by properties individual material properties of both the materials. From the obtained stretch and stress, the equivalent material property of combined matrix and carbon nanotube is achieved. This property is provided as input in simple rule of mixtures to find out the equivalent orthotropic materials are determined. It is inferred that experiment results are in good agreement with results generated by ANSYS. The superiority of the presence of carbon nanotube in the composite is proved from experimental and finite element technique from the estimated fracture parameters.

Keywords – *Carbon epoxy, carbon nanotube, FEA, ILSS*

1. INTRODUCTION

In aeronautical industry carbon fiber reinforced polymeric composites are used to manufacture several components such as flaps, aileron, landing – gear doors and others [1]. The mechanical property of the composite becomes complex with the addition of fibers. When subjected to compression, tension and flexure tests polymeric composites are susceptible to mechanical damages that can lead to interlayer delamination. Catastrophic failure of the component can occur due to the increase in the external load [2]. Mechanical evaluation is essential to minimize these failures in aircraft parts. In 1991, Iijima

[3] discovered carbon nanotubes while performing experiment on synthesis of fullerenes with arch discharge method. Multiwalled and single walled carbon nanotubes were his inventions [6]. Researchers envisioned them as the prime candidates to dominate the revolution in nanotechnology. Carbon nanotubes have large aspect ratio, low density and high strength and modulus. Therefore, they are ideal candidates for reinforcement [4 - 7].

Based on classical laminated plate theory and first order shear deformation theory non linear post buckling results were obtained for finite element model. Experimentally observed failure mode was substantiated with their results. End Notched Flexure specimen with sufficiently long bond length was used to estimate interface shear fracture by Zhenyu Ouyang et al [8] for cohesive zone model based on an analytical solution. To enhance the interlaminar shear fracture toughness Daniel C Davis et al [9] demonstrated that fluorine functionalized CNTs can be used to reinforce the midplane of a fiber reinforced epoxy composite laminate. Transverse stitching [10,11] or pinning [12,13] the fabric across the laminate to hold the plies together to increase interlaminar shear strength under physical approach. Interlaminar shear strength was obtained from ASTM C 1425 [14]. The experiments were conducted for carbon epoxy composite and carbon epoxy carbon nanotube composites. Mechanical properties such as thickness and elastic ratios are varied to examine the interlaminar shear strength in carbon epoxy and carbon epoxy carbon nanotube by ANSYS.

2. PROBLEM FORMULATION

The objective of the present work is to estimate interlaminar shear strength in carbon epoxy and carbon nanotube composites using experimental and finite

element technique. Experiments are conducted as per ASTM standards. Finite element model is generated in ANSYS and comparison of the results is made.

3. METHODOLOGY

3.1 Experimental methodology

Hand layup process is used to fabricate carbon epoxy composite. Percentage of volume fraction of void content, fiber and matrix are determined from ASTM D 3171 [15]. To make the carbon nanotubes disperse completely in matrix, ball milling is done to disperse carbon nanotubes in matrix. Hand layup process is used to fabricate the carbon epoxy carbon nanotube composite. Sample and notch dimensions are made as per the dimensions mentioned in ASTM C 1425 [14] are shown in table 3.1 and table 3.2. Fixture is also fabricated with three sets of semi cylindrical spacers to make the sample fit inside the fixture. Fixture for estimating interlaminar shear strength consists of top piston, bottom piston, hollow cylinder and semi cylindrical spacers. The samples are shown in Fig. 3.1. The assembled view of the fixture is shown in Fig. 3.2. Detailed drawing of the specimen with dimension is shown in Fig. 3.3. The appearance of the samples after fracture is shown in Fig. 3.4. The samples are subjected to loading and interlaminar shear strength is estimated.

SNo	Date	Sample dimension in mm			
		Length	Width	Thickness	Distance between notches
1	S2 30/10/09	30.98	14.88	2.01	5.9
2	S1 30/10/09	30.11	14.88	2.13	5.91
3	S2 30/10/09	30.1	14.64	2.06	5.88
4	S2 12/11/09	30.03	14.76	2.37	5.84
5	S1 12/11/09	29.93	14.59	1.98	5.87
6	S2 30/10/09	29.86	14.88	2.03	5.95
Average value		30.16	14.77	2.09	5.89

Table 3.1 Samples dimensions of double notched specimen in carbon epoxy composite

		With label (Face 1)		Without label (Face 2)	
S.No	Date	Width (mm)	Depth (mm)	Width (mm)	Depth (mm)
1	S1 12/11/09	0.34	1	0.33	0.84
2	S1 30/10/09	0.35	1.09	0.36	1
3	S2 30/10/09	0.39	1	0.53	1.09
4	S2 12/11/09	0.39	0.6	0.45	0.86
5	S2 30/10/09	0.43	0.91	0.42	0.99
6	S2 30/10/09	0.45	0.91	0.3	0.59
Average		0.39	0.92	0.4	0.89

Table 3.2 Notch width and depth dimensions of double notched specimen in carbon epoxy composite

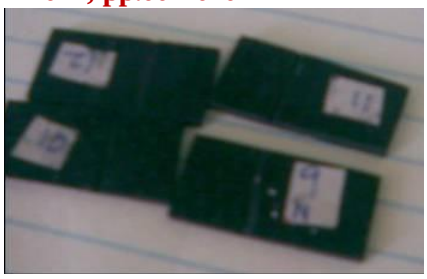

Figure 3.1 Double notch specimens

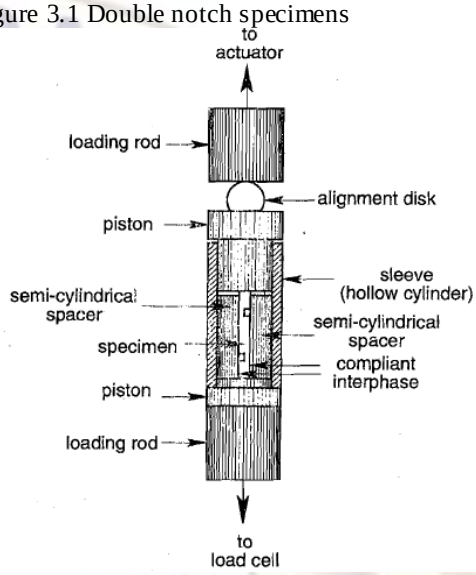

Figure 3.2 Assembled view of the fixture

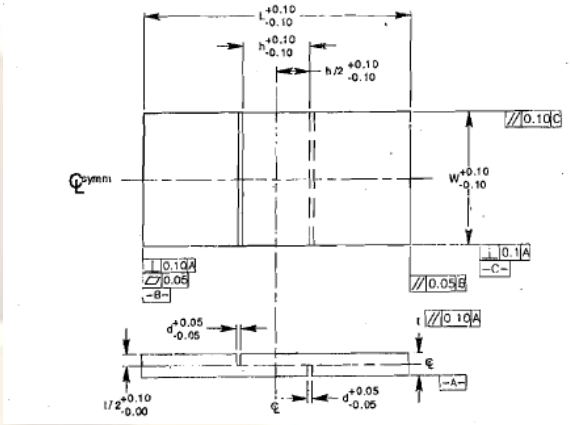

Figure 3.3 Double notched specimen

SNo	Date	V_v	V_f	V_m
1	S2 30/10/09	0.03283	0.57446	0.3927
2	S2 30/10/09	0.03283	0.57446	0.3927
3	S2 30/10/09	0.03283	0.57446	0.3927
4	S2 12/11/09	0.03818	0.5693	0.3924
5	S1 12/11/09	0.05363	0.5691	0.37719
6	S1 30/10/09	0.00686	0.5471	0.44603
Average		0.03286	0.5681	0.3989

Table 3.3 Volume fractions in double notched specimen in carbon epoxy composite

The volume fraction in carbon epoxy carbon nanotube is estimated using ASTM 3171 [15]. One percent of the matrix is taken as one percentage of matrix since one weight percentage of CNT's are added to the matrix while making resin. The volume fraction of fiber, matrix, carbon nanotube and void content are 0.62, 0.33, 0.0033 and 0.04 respectively.

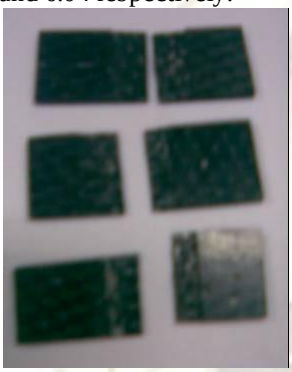

Figure 3.4 Double notched specimens after fracture

All the samples fractured at the gage section and hence it is concluded that the test is valid.

SNo	Sample dimension mm			Distance between notches
	Length	Width	Thickness	
1	30.02	14.47	2.04	6.45
2	30.09	14.46	2.1	8.36
3	30.12	14.66	2.06	7.53
4	30.15	14.72	2.06	7.63
5	30.3	14.54	1.97	5.98
Avg	30.13	14.57	2.05	7.19

Table 3.4 Sample dimensions of double notched specimen in carbon epoxy CNT composite

	With label (Face1) mm		With label (Face 2) mm	
S.No	Depth	Width	Depth	Width
1	0.67	0.77	0.85	0.83
2	0.67	0.57	0.69	0.52
3	0.88	0.39	0.99	0.54
4	0.93	0.61	0.98	0.55
5	1	0.35	1	0.64
Avg	0.83	0.54	0.916	0.62

Table 3.5 Dimensions of the notch in double notched specimen in carbon epoxy cnt composite

3.2 Finite element Method

Micromechanics procedure [16] is discussed for estimating the material properties of composite used in present study.

Material	Properties	Value
Carbon fiber	Elastic Modulus (GPa)	220
	Shear Modulus (GPa)	25
	Density (g/cc)	1.7
	Poisson's ratio	0.15
Epoxy Resin	Elastic Modulus (GPa)	3.3
	Shear Modulus (GPa)	1.2
	Density (g/cc)	1.2
	Poisson's ratio	0.37

Table 3.6 Properties of carbon fiber and epoxy resin

Table 3.6 shows the mechanical properties of constituents of test specimen used. Elastic constants of unidirectional composite are calculated using simple rule of mixtures. After calculating elastic constants of the unidirectional composite, elastic constants of woven fabric composite material are estimated using the equations 3.7 to 3.12. The elastic constants using the equations discussed earlier in this section are provided in table 3.5 with reference to volume fraction of fiber. Upon providing the material properties as input, double notched specimen is modeled in ANSYS and the results are discussed later part of paper in comparison with the experiments conducted.

$$E_1 = E_f V_f + E_m(1-V_f) \quad (3.1)$$

$$E_2 = E_m\left[\frac{E_f + E_m + (E_f - E_m)V_f}{E_f + E_m - (E_f - E_m)V_f}\right] \quad (3.2)$$

$$\nu_{12} = \nu_f V_f + \nu_m(1-V_f) \quad (3.3)$$

$$\nu_{23} = \nu_f V_f + \nu_m(1-V_f)\left[\frac{1+\nu_m - \nu_{12}\left(\frac{E_m}{E_{11}}\right)}{1-\nu_m{}^2 + \nu_m\nu_{12}\left(\frac{E_m}{E_{11}}\right)}\right] \quad (3.4)$$

$$G_{12} = G_m\left[\frac{G_f + G_m + (G_f - G_m)V_f}{G_f + G_m - (G_f - G_m)V_f}\right] \quad (3.5)$$

$$G_{23} = \frac{E_{22}}{2(1+\nu_{23})} \quad (3.6)$$

where m and f denote matrix and fiber respectively

$$\left[\frac{2}{E_1}\frac{E_1(E_1+(1-\nu^2{}_{12})E_2)-\nu^2{}_{12}E^2{}_2}{E_1(E_1+2E_2)+(1+2\nu^2{}_{12})E^2{}_2}\right]^{UD} = \left(\frac{1}{E_1}\right)^{WF} \quad (3.7)$$

$$\left[\frac{4}{E_1}\frac{\nu_{12}E_2(E_1-\nu^2{}_{12}E_2)}{E_1(E_1+2E_2)+(1+2\nu^2{}_{12})E^2{}_2}\right]^{UD} = \left(\frac{\nu_{12}}{E_1}\right)^{WF} \quad (3.8)$$

$$\left[\frac{1}{E_1}\frac{E_1(\nu_{12}+\nu_{23}+\nu_{12}\nu_{23})+\nu^2{}_{12}E_2}{E_1+(1+2\nu_{12})E_2}\right]^{UD} = \left(\frac{\nu_{13}}{E_1}\right)^{WF} \quad (3.9)$$

$$\left[\frac{(1-\nu_{23}{}^2)E_1{}^2+(1+2\nu_{12}+2\nu_{12}\nu_{23})E_1E_2-\nu^2{}_{12}E^2{}_2}{E_1E_2(E_1+(1+2\nu_{12})E_2)}\right] = \left(\frac{1}{E_3}\right)^{WF} \quad (3.10)$$

$$\left(\frac{1}{G_{12}}\right)^{UD} = \left(\frac{1}{G_{12}}\right)^{WF} \quad 3.11)$$

$$\left(\frac{1+\nu_{23}}{E_2}+\frac{1}{2G_{12}}\right)^{UD} = \left(\frac{1}{G_{13}}\right)^{WF} \quad 3.12)$$

The element used for generating this sample is layered solid 46 [17]. The element is defined in three dimensional space with eight nodes and three degrees of freedom ux, uy and uz at each node. Fig. 3.3 shows the finite element mesh of double notched specimen. The mesh has 4904 nodes and 3600 elements. Fig. 3.3 shows the finite element mesh of double notched specimen at the vicinity of the crack tip.

Elastic constant	Vf @0.57	Vf @0.56	Vf @0.56	Vf @0.54
E1 (GPa)	70.03	66.71	69.38	69.31
E2 (GPa)	70.03	66.71	69.38	69.31
E3 (GPa)	12.65	11.72	12.47	12.47
υ12	0.04	0.043	0.04	0.04
υ23	0.31	0.34	0.31	0.3
υ13	0.31	0.34	0.31	0.3
G12 (GPa)	3.81	3.57	3.77	3.76
G23 (GPa)	4.19	4.03	4.16	4.15
G13 (GPa)	4.19	4.03	4.16	4.15

Table 3.7 Elastic constants at different volume fractions of fiber

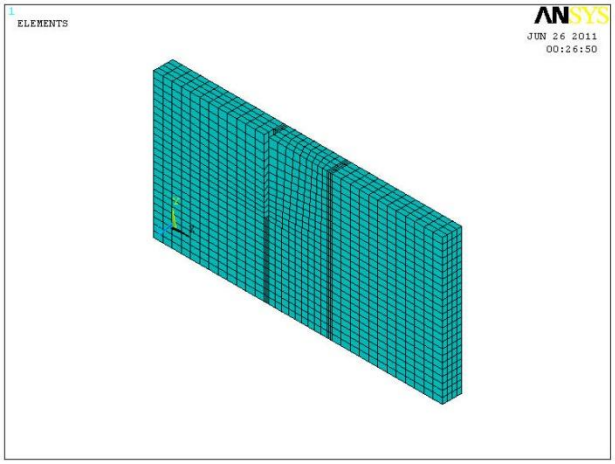

Figure 3.2 Finite element mesh of double notched specimen

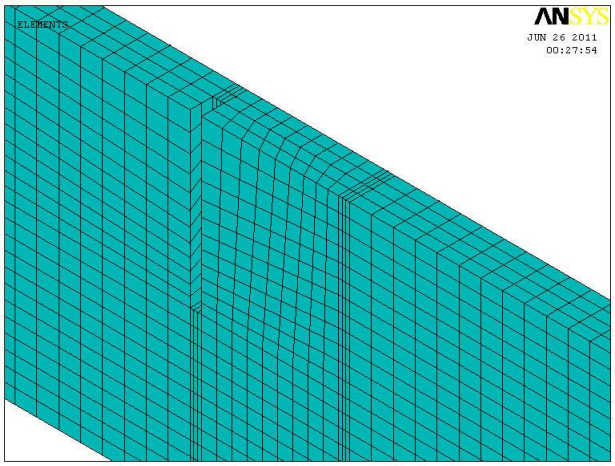

Figure 3.3 Finite element mesh of double notched specimen at the vicinity of the crack tip

Matrix	Property / Geometric dimension	Value
	Young's modulus GPa	3
	Poisson's ratio	0.37
	Matrix diameter nm	45
	Matrix length nm	4000
MWCNT	Young's modulus TPa	2
	Poisson's ratio	0.23
	cnt inside diameter nm	1.5
	cnt length nm	25
	cnt diameter nm	3.38

Table 3.8 Properties and geometric dimensions of CNT

Equivalent material properties of matrix and nanotube are estimated [16]. From elastic constants and geometric dimensions of matrix and CNT finite element model is generated with suitable boundary conditions and loading to get young's modulus and poisson's ratio. The properties and geometric dimensions of matrix and CNT used in the present work are mentioned in table 3.8. Axial stretch case is considered in the present work to estimate the equivalent material properties.

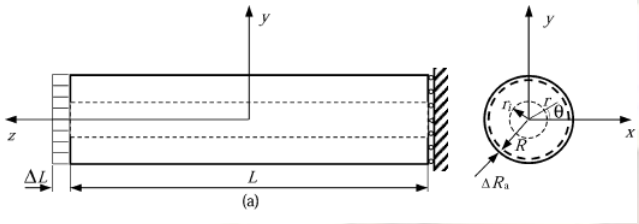

Figure 3.4 Axial stretch case

Cylindrical representative volume element concept is used to model finite element model concept and is shown in Fig 3.4 [18]. Plane 82 and solid 45 [17] are the elements used to model matrix and carbon nanotube. Plane 82 has 4 corner nodes and 4 mid side nodes with two translational degrees of freedom along X and Y directions at each node. Plane strain assumption is selected under element behaviour option. Upon meshing, solid 45 element is used to generate three dimensional model. Solid 45 has 8 nodes with three translational degrees of freedom along X, Y and Z axes. The finite element model is shown in Fig. 3.5. At a load of 140 MPa, carbon nanotube and matrix finite element model showed an axial stretch of 20.481 nm and is shown in Fig. 3.6. From the equation $\varepsilon_z = \frac{\delta}{l}$ axial strain along Z direction is estimated.

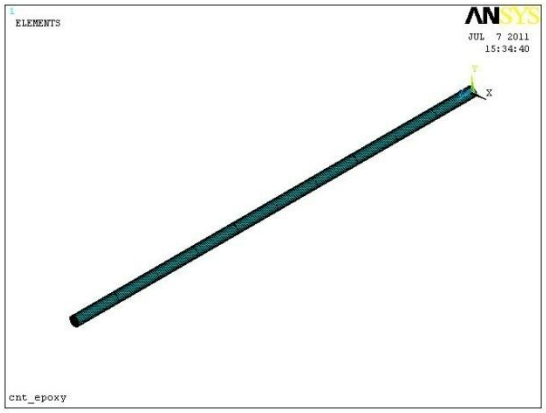

Figure 3.5 Finite element model of carbon nanotube and matrix

Also axial stress along Z direction is determined from finite element analysis from axial stress distribution and is shown in Fig. 3.7. From the equation $E_z = \frac{\sigma_z}{\varepsilon_z}$ young's modulus is estimated. To find poisson's ratio, radial displacement and axial displacement are required. The distribution of radial displacement is shown in Fig. 3.8. From the relation $G_{zx} = \frac{E_z}{2(1+\nu_{zx})}$ shear modulus is estimated.

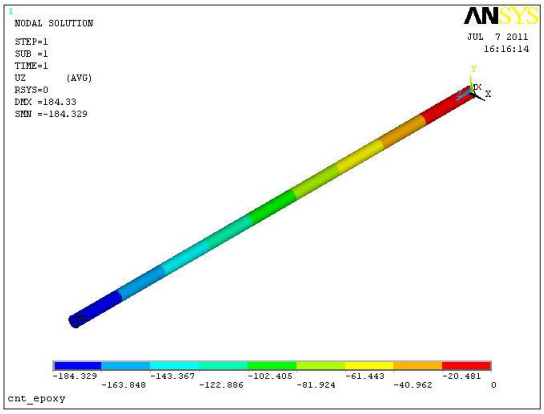

Figure 3.6 Axial stretch distributions in nm

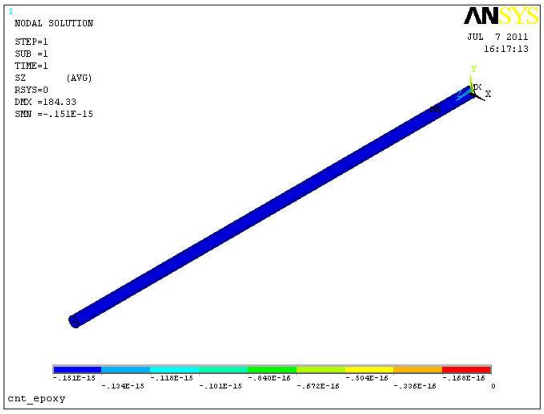

Figure 3.7 Axial stress distribution in Nnm^{-2}

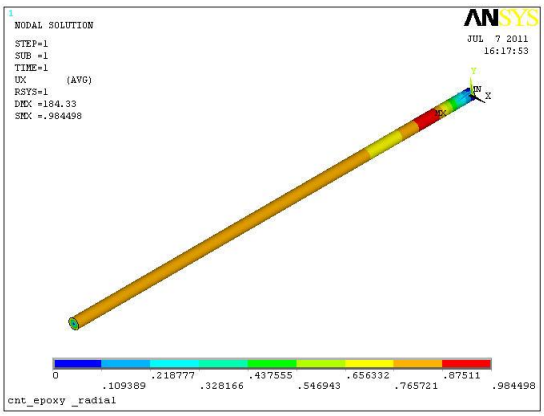

Figure 3.8 Radial displacement distributions in nm

In the present work to fabricate composite 0.579 g of carbon nanotube is used. Comparison between theoretical and experimental carbon nanotube weight and young's

modulus is made to estimate the experimental young's modulus. Theoretical carbon nanotube weight is determined from the relation $\omega_{cnt} = V_{cnt} \times \rho_{cnt}$ where density of carbon nanotube is 1.8 g/cc. In the equation $V_{cnt} = \frac{r_o^2 - r_i^2}{R^2 - r_i^2}$ r_o is the outer radius of carbon nanotube, r_i is the inner radius of carbon nanotube and R is the matrix radius. V_{cnt} value is found to be 0.3079. Therefore the theoretical weight of carbon nanotube is 0.554 g. The corresponding young's modulus for theoretical weight is obtained from finite element analysis performed in ANSYS whose value is 3.2812 GPa. For 0.579 g of carbon nanotube 3.4292 GPa will be the corresponding young's modulus which is used while fabricating the composite. The material properties obtained are mentioned in table 3.9

Elastic constant	Vf @0.62
E1 (GPa)	76.4
E2 (GPa)	76.4
E3 (GPa)	15.69
υ12	0.04
υ23	0.85
υ13	0.85
G12 (GPa)	4.19
G23 (GPa)	4.53
G13 (GPa)	4.53

Table 3.9 Estimated Elastic constants

Elastic constant	Vf @0.50	Vf @0.60	Vf @0.70
E1 (GPa)	60.93	73.29	86.59
E2 (GPa)	60.93	73.29	86.59
E3 (GPa)	10.55	13.49	18.22
υ12	0.039	0.039	0.04
υ23	0.67	0.66	0.68
υ13	0.67	0.66	0.68
G12 (GPa)	3.19	4.07	5.39
G23 (GPa)	3.34	4.39	6.01
G13 (GPa)	3.34	4.39	6.01

Table 3.10 Estimated Elastic constants at different volume fractions of fiber in carbon epoxy composite

Elastic constant	Vf @0.80	Vf @0.90
E1 (GPa)	102.04	124.64
E2 (GPa)	102.04	124.64
E3 (GPa)	27.08	49.57
υ12	0.048	0.065
υ23	0.74	0.98
υ13	0.74	0.98
G12 (GPa)	7.58	11.95
G23 (GPa)	8.87	15.14
G13 (GPa)	8.87	15.14

Table 3.11 Estimated Elastic constants at different volume fractions of fiber in carbon epoxy composite

The elastic constants are estimated using the equations mentioned in chapter 5 for volume fraction of fiber from 50 % to 90 %. The values of these constants are shown in table 7.1 a and 7.2 b.

Elastic constant	Vf @0.50	Vf @0.60	Vf @0.70
E1 (GPa)	63.27	74.15	85.14
E2 (GPa)	63.27	74.15	85.144
E3 (GPa)	15.72	15.86	16.06
υ12	0.062	0.05	0.04
υ23	1.11	0.94	0.78
υ13	1.11	0.94	0.78
G12 (GPa)	3.95	4.15	4.36
G23 (GPa)	4.1	4.44	4.8
G13 (GPa)	4.1	4.44	4.8

Table 3.12 Estimated elastic constants at different volume fractions of fiber in carbon epoxy carbon nanotube composite

The elastic constants are determined using equations mentioned under the heading three for fiber volume fraction varying from 0.5 to 0.9. The values of the elastic constants are shown in table 3.11 and 3.12

4. RESULTS AND DISCUSSIONS

In this section, interlaminar shear strength is estimated using experimental and finite element technique is presented. Firstly, interlaminar shear strength distribution with variation in load for double notched specimen for carbon epoxy and carbon epoxy carbon nanotube composite are listed in tables 4.1 and 4.2.

SNo	P_{max} in N	Interlaminar shear strength in MPa		Deviation in %
		ANSYS	Experiment	
1	2210	22.72	24.99	9.058
2	2418	24.86	28.05	11.35
3	2732	28.09	31.89	11.92
4	2834.7	29.15	32.23	9.56
5	3250	33.42	35.82	6.69
6	3502	36.01	38.97	7.58
Avg	2824.45	29.04	31.99	9.21

Table 4.1 Interlaminar shear strength in carbon epoxy composite with variation in load

Table 4.1 shows the distribution of interlaminar shear strength for carbon epoxy composite with variation in load. Along the tension side, the estimated interlaminar shear strength values from ANSYS and experiment are 36.01 MPa and 38.973 MPa respectively. While along the compression side, the interlaminar shear strength values from experiment and ANSYS are 24.99 MPa and 22.72

MPa respectively. It is observed that there is variation in interlaminar shear strength with variation in load keeping the volume fraction of the fiber constant while performing finite element analysis. The estimated volume fraction of fiber varies from 0.54 to 0.57 during experimental analysis. The fabricated notch dimensions have effect on the estimated interlaminar shear strength values obtained from experiment and hence there is deviation in the values observed.

SNo	P_{max} in N	ILSS in MPa		Deviation in %
		ANSYS	Experiment	
1	5059	48.775	45.82	6.04
2	5580	53.798	64.17	19.28
3	6496.3	62.629	53.73	14.19
4	6719	64.779	71.99	11.13
5	7240	69.802	64.46	7.64
Average	6218.86	60.03	59.95	0.5

Table 4.2 Interlaminar shear strength in carbon epoxy carbon nanotube composite with variation in load

From table 4.2 it is seen that there is variation in interlaminar shear strength with variation in load. Along tension and compression side the experimental values of interlaminar shear strength are 45.82 MPa and 71.99 MPa respectively. From finite element analysis the estimated tensile and compressive values of interlaminar shear strength are 48.77 MPa and 69.8 MPa. As mentioned under the discussion part of table 1, same reasonings also apply for the experimental observed values of interlaminar shear strength. It is important to note that there is improvement in the interlaminar shear strength when carbon nanotubes are dispersed in matrix and composite is fabricated from it.

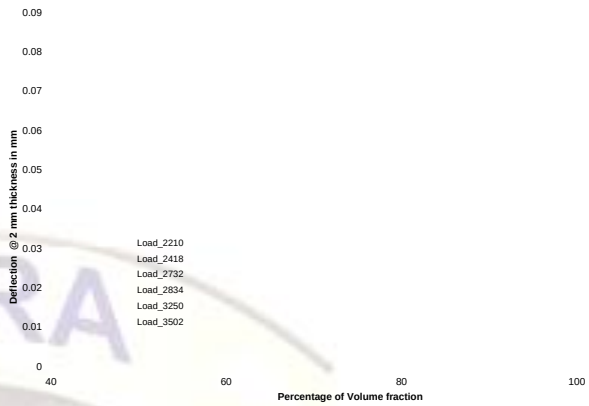

Figure 4.1 Variation of deflection with variation in load by increase in percentage of volume fraction

Figure 4.2 Variation of interlaminar shear strength with variation in load by increase in percentage of volume fraction

Fig. 4.1 and 4.3 examine the variation of deflection at thickness of 2 mm and 3 mm with increase in percentage of volume fraction. It is observed that there is variation in deflection due to variation in load. Tensile values of deflection are observed at compressive percentages of volume fraction keeping the applied load constant. At compressive percentage of volume

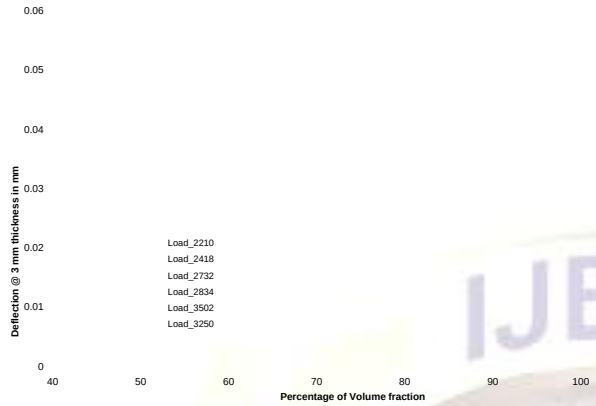

Figure 4.3 Variation of deflection with variation in load by increase in percentage of volume fraction

Figure 4.4 Variation of interlaminar shear strength with variation in load by increase in percentage of volume fraction

fraction, the amount of fiber consumed in fabricating the composite is less. Since the amount of fiber is less, there is scope for more amount deflection observed. In general, in a composite consisting of more amount of fiber, there is less chance for pull out. Therefore it can be concluded that fibers obstruct the deformation along the direction of applied load.

Fig. 4.2 and 4.4 show the variation of interlaminar shear strength at thickness of 2 mm and 3mm with increase in percentage of volume fraction. From the figure it can be seen that variation in load produces variation in interlaminar shear strength. Keeping the load constant, the influence of percentage of volume fraction of interlaminar shear strength can be analysed. From 0.4 to 0.57 percentage of volume fraction there is a rise in ILSS. At 0.6 there is a fall in ILSS value and from 0.7 to 0.8 there is again a rise in the values of ILSS. The compressive value of ILSS is observed at 0.9 percentage of volume fraction. This value is less in comparison with that of percentage of volume fraction at 0.4. From these inferences it is concluded that fibers and notch dimensions arrest the observed values of interlaminar shear strength.

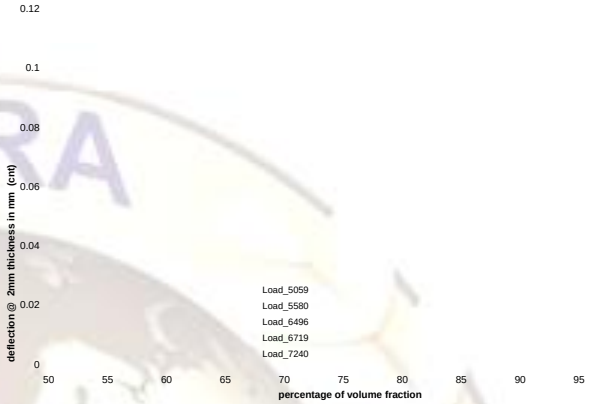

Figure 4.5 Variation of deflection with variation in load by increase in percentage of volume fraction

Figures 4.5 and 4.7 examine the variation of deflection at thickness of 2 mm and 3 mm with increase in percentage of volume fraction. Due to variation in load there is variation in deflection. Keeping load constant it is noticed that peak values of deflections are observed at 0.62 percentage of volume fraction. Compressive deflections are seen at compressive percentages of volume fraction while applied load is constant. This implies that in addition to fiber, carbon nanotubes also obstruct the deformations that are generated.

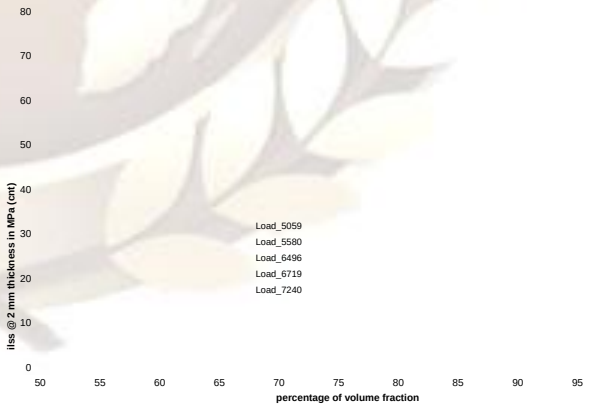

Figure 4.6 Variation of interlaminar shear strength with variation in load by increase in percentage of volume fraction

For the elastic constants mentioned in table 3.11 and 3.12 the interlaminar shear strength is estimated. Effect of

thickness on the interlaminar shear strength is shown in the graphs.

Fig. 4.6 and 4.8 shows the variation of interlaminar shear strength at thickness of 2 mm and 3mm with increase in percentage of volume fraction. Variation in interlaminar shear strength is seen with variation in percentage of volume fraction. The influence of percentage of volume fraction of interlaminar shear strength can be examined keeping the load constant. Tensile interlaminar shear strength is observed at 0.62 percentage of volume fraction.

Figure 4.7 Variation of deflection with variation in load by increase in percentage of volume fraction

Figure 4.8 Variation of interlaminar shear strength with variation in load by increase in percentage of volume fraction

5. CONCLUSIONS

1. The finite element analysis results are compatible with experimental results
2. The equations mentioned in under heading three gave compatible results.
3. The appearance of the specimen after fracture showed expected behavior. All the samples fractured at the gage section as mentioned in the standard.
4. In carbon epoxy composite fabricated to estimate interlaminar shear strength, experiment and finite element technique are used. From experiment, 31.99 MPa was obtained while from finite element technique 29.04 MPa was obtained. The deviation observed from both the methods is 9.36 %.
5. It was also noticed that as load increases, interlaminar shear strength increases and vice versa
6. In carbon epoxy carbon nanotube composite, interlaminar shear strength was estimated. Experiment gave a value of 59.95 MPa and ANSYS gave a value of 60.04 MPa respectively with a deviation of 0.5 %.
7. From 4 and 6 it is inferred that carbon epoxy carbon nanotube composite gave higher interlaminar shear strength value in comparison with carbon epoxy composite. Therefore it can be said that carbon epoxy carbon nanotube is a superior material in comparison with carbon epoxy material.
8. Also it is inferred that distance between the notches during fabrication effects the interlaminar shear strength while conducting experiment.
9. Mechanical properties such as elastic constants and thickness are varied to estimate deflections and interlaminar shear strength in carbon epoxy and carbon epoxy carbon nanotube composites.
10. Keeping the applied load constant in carbon epoxy composite, tensile values of deflection are observed at compressive percentages of volume fraction.
11. Peak value of interlaminar shear strength was observed at 0.8 percentage of volume fraction in carbon epoxy composite
12. Compressive deflections are seen at compressive percentages of volume fraction while applied load is constant and therefore it is concluded that addition of carbon nanotubes to matrix and the presence of fiber obstruct the deformations that are generated in carbon epoxy carbon nanotube composite.
13. At compressive percentage of volume fraction, compressive interlaminar shear strength is seen. The interlaminar shear strength appears to be linear from 0.62 to 0.9 percentage of volume fraction of the fiber.

6. ACKNOWLEDGEMENTS

The authors would like to thank Dr. Rohini Devi, Shri Anil Kumar and Shri I. Srikanth of Advanced System Laboratory, Hyderabad for their advice and help provided during the experimental work.

REFERENCES

1. Schwartz MM, "Composite materials: Properties, Nondestructive testing and Repair" Volume 1 New Jersey, USA, Prentice Hall Inc 1997
2. Kim J, Shioya M, Kobayashi H, Kaneko J, Kido M "Mechanical properties of woven laminates and felt composites using carbon fibers Part 1: in-plane properties" Composite Science and Technology, 2004, 64, 2221 – 2229
3. S.Iijima, Nature 354 (1991) 56 – 58
4. Qian D et al , "Load transfer and deformation mechanisms in carbon nanotube – polystyrene composites " Appl Phys Lett 2000 , 76 (20) 2868 – 70
5. Lourie O et al , "Transmission electron microscopy observations of fracture of single wall carbon nanotubes under axial tension " Appl Phys Lett 1998 73 (24) 3527 – 9
6. Cooper C A et al , "Detachment of nanotubes from a polymer matrix" Appl Phys Lett 2002, 81 (20) : 3873 – 75
7. Thostenson E T et al, "Aligned multiwalled carbon nanotube reinforced composites : processing and mechanical characterization" J Phys D Appl Phys 2002, 35, 77 - 80
8. Ouyang Z et al, 2009, Cohesive zone model based analytical solutions for adhesively bonded pipe joints under torsional loading. International Journal of Solids and Structures 46 (5), 1205 - 1217
9. Gojny FH et al, "Carbon nanotube reinforced epoxy composites: enhanced stiffness and fracture toughness at low nanotube content" Compos Sci Technol, 2004, 64 : 2363 – 71
10. Shu D et al, Effect of stitching on interlaminar delamination extension in composite laminates, Composite Science Technology 1993, 49 , 165 – 71
11. Chen L et al, "A novel double cantilever beam test for stitched composite laminates" Journal of composite material 2001, 35 (13): 1137 – 49
12. Liu et al, "Delamination fracture mechanics of composite laminate with through thickness pinning" Strength Fract Complex 2003, 1 (3), 139 – 146
13. Lenzi et al, "coupon tests on z – pinned and unpinned composite samples for damage resistant applications " Macromol Sympos Times Polym Compos 2007; 27 (1), 230 – 7 (Special Issue)
14. ASTM C1425 – 05 Standard test method for interlaminar shear strength of 1-D and 2-D continuous fiber-reinforced advanced ceramics at elevated temperatures
15. ASTM D 3171 – 09 Standard test methods for constituent content of composite materials
16. MF Aly et al, "Experimental investigation of the dynamic characteristics of laminated composite beams" , International Journal of Mechanical and Mechatronics Vol 10, No 3, 59 - 68
17. ANSYS 9.0 Element library of ANSYS
18. YJ Liu and XL Chen, "Evaluations of the effective material properties of carbon nanotube based composites using a nanoscale representative volume element", Mechanics of materials, 35 (2003), 69 – 81